

Preparation, Characterization, Cytotoxicity, and Genotoxicity Evaluations of Thiolated- and S-Nitrosated Superparamagnetic Iron Oxide Nanoparticles: Implications for Cancer Treatment

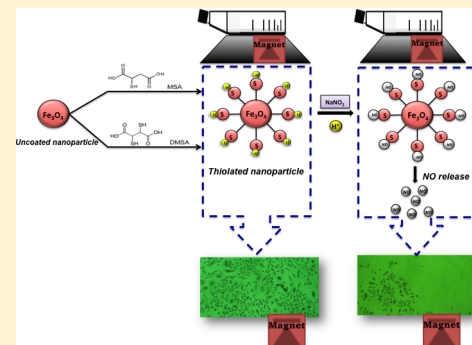
Amedea B. Seabra,^{*,†} Tatiane Pasquôto,[‡] Ana Carolina F. Ferrarini,[†] Marconi da Cruz Santos,[†] Paula S. Haddad,[†] and Renata de Lima[§]

[†]Exact and Earth Sciences Department, Universidade Federal de São Paulo, Diadema, São Paulo 09913030, Brazil

[‡]Universidade Federal de São Carlos, UFSCar, Sorocaba, São Paulo 18052780, Brazil

[§]Department of Biotechnology, Universidade de Sorocaba, Sorocaba, São Paulo 18023000, Brazil

ABSTRACT: Iron oxide magnetic nanoparticles have been proposed for an increasing number of biomedical applications, such as drug delivery. To this end, toxicological studies of their potent effects in biological media must be better evaluated. The aim of this study was to synthesize, characterize, and examine the potential *in vitro* cytotoxicity and genotoxicity of thiolated (SH) and S-nitrosated (S-NO) iron oxide superparamagnetic nanoparticles toward healthy and cancer cell lines. Fe_3O_4 nanoparticles were synthesized by coprecipitation techniques and coated with small thiol-containing molecules, such as mercaptosuccinic acid (MSA) or meso-2,3-dimercaptosuccinic acid (DMSA). The physical–chemical, morphological, and magnetic properties of thiol-coating Fe_3O_4 nanoparticles were characterized by different techniques. The thiol groups on the surface of the nanoparticles were nitrosated, leading to the formation of S-nitroso-MSA- or S-nitroso-DMSA- Fe_3O_4 nanoparticles. The cytotoxicity and genotoxicity of thiolated and S-nitrosated nanoparticles were more deeply evaluated in healthy (3T3, human lymphocytes cells, and Chinese hamster ovary cells) and cancer cell lines (MCF-7). The results demonstrated that thiol-coating iron oxide magnetic nanoparticles have few toxic effects in cells, whereas S-nitrosated-coated particles did cause toxic effects. Moreover, due to the superparamagnetic behavior of S-nitroso- Fe_3O_4 nanoparticles, those particles can be guided to the target site upon the application of an external magnetic field, leading to local toxic effects in the tumor cells. Taken together, the results suggest the promise of S-nitroso-magnetic nanoparticles in cancer treatment.



1. INTRODUCTION

Over the past decade, there has been a growing interest in the development of smart and biocompatible nanomaterials with different chemical and physical properties for a wide range of biomedical and technological applications.^{1–5} Among the promising nanostructured materials, iron oxide magnetic nanoparticles, in particular magnetite (Fe_3O_4), have attracted the attention of the scientific community.^{6,7} Indeed, magnetic nanoparticles have been successfully used in different biomedical applications, such as in diagnosis,⁸ drug delivery,^{9,10} and hyperthermia.¹¹ Each nanoparticle shows superparamagnetic behavior when the temperature is above the so-called blocking temperature and acts as a single magnetic domain. Such individual nanoparticles have a large constant magnetic moment and behave as a giant paramagnetic atom, quickly responding to applied magnetic fields with negligible residual magnetism and coercivity.¹²

To propose safe biomedical applications of iron-based magnetic nanoparticles, caution must be taken regarding the biocompatibility of these nanoparticles. The information reported in the literature concerning the toxicity of iron oxide magnetic nanoparticles may be conflicting. As a function

of the chemical nature of their coating, Fe_3O_4 magnetic nanoparticles do not have the same behaviors in biological systems.¹³ For instance, depending on the nanoparticles, they can be internalized into cells or attached onto the cell membranes, leading to cell death or cell proliferation.¹⁴ Uncoated iron-based magnetic nanoparticles induce a dramatic decrease in the metabolic activity and proliferation of human cells.¹⁵ However, the coating of those nanoparticles seems to be of great importance with regard to cell adhesion, internalization efficiency, and cytotoxic effects.^{16,17} Usually, coated magnetic nanoparticles have been found to be nontoxic, whereas the bare particles exert some toxic effects.¹⁸

meso-2,3-Dimercaptosuccinic acid (DMSA) is one of the most widely used coating molecules for magnetic nanoparticles, increasing cell internalization¹⁹ and biocompatibility.²⁰ Important studies have confirmed that DMSA-coated iron oxide magnetic particles can greatly enhance the rate of cellular uptake, leading to a nonspecific adsorption to the cell surface, followed by endocytosis into the cell.^{21,22} Recently, Mejias et

Received: March 24, 2014

Published: June 20, 2014



al.²⁰ reported that DMSA-coated magnetic nanoparticles have little effect on cell viability, oxidative stress, cell cycle, or apoptosis in NTC 1469 nonparenchymal hepatocytes cells *in vitro*. Similarly, our group reported that mercaptosuccinic acid (MSA) can also be used to coat magnetic Fe₃O₄ nanoparticles with no cytotoxic effects.^{23,24}

Coating nanoparticles with such molecules as DMSA or MSA may not only increase the biocompatibility of these systems but also represent a strategy to conjugate active molecules to the nanoparticle's surface. Drug delivery is employed to carry important active molecules in a region-specific manner by attaching them to the large surface area of the magnetic nanoparticle, releasing the drug in the biological system directly at the local target.^{21,25} The thiol groups present in MSA or DMSA can be nitrosated, leading to the formation of S-nitroso-MSA- and S-nitroso-DMSA-Fe₃O₄ magnetic nanoparticles, respectively. The formation of S-nitroso-groups (S-nitrosothiols) on the surface of Fe₃O₄ nanoparticles leads to nitric oxide (NO)-releasing iron oxide magnetic nanoparticles, as previously reported by our group.^{23,24,26}

NO is a key molecule in the biological system due to its small size, chemical instability, and relative lipophilicity. NO is an important molecule that is involved in such physiological processes as the dilation of blood vessels, inhibition of platelet adhesion and aggregation, cell communication, wound healing, immune responses, apoptosis, and anticancer activities.^{23,24,27–32} However, the potential therapeutic applications of NO have been limited by its instability and potential systemic effects exerted *in vivo*.³³ In this context, there is a need to develop NO donors with potent antiproliferative properties and minimal side effects.^{1,34} The major goal of NO-based therapy is the development of a NO-releasing material capable of releasing optimal amounts of NO at the desired flux directly to the target site of application, where NO can have its therapeutic effects.^{1–3} In this scenario, iron oxide magnetic nanoparticles represent a promising vehicle for the storage and local delivery of active amounts of NO. NO-releasing iron oxide nanoparticles may have applications in anticancer therapies. These nanostructured systems also show great potential to transform the future of cancer theranostics, which is the combination of diagnosis and healing approaches in cancer treatment.³⁵ Most cancer drugs are cytotoxic due to a lack of targeting specificity; these drugs can diffuse into the neighboring tissues and damage them. Magnetic nanoparticles with better targeting and low cytotoxicity have been developed recently to avoid this problem.^{23–25}

In this work, iron oxide (Fe₃O₄) magnetic nanoparticles were synthesized and coated with small thiol-containing molecules, either MSA or DMSA, leading to thiolated nanoparticles. The morphology, physical-chemical, and magnetic properties of the compounds are characterized by different techniques. Thiol groups on the surface of MSA- or DMSA-coated Fe₃O₄ were nitrosated, leading to the formation of S-nitroso-MSA or S-nitroso-DMSA nanoparticles, which act as NO donors.²⁶ To propose a biomedical application of S-nitrosated magnetic nanoparticles, the cytotoxicity and genotoxicity of the systems were investigated in healthy and MCF-7 breast cancer cell lines. Moreover, the magnetic properties of S-nitrosated nanoparticles can be used as a tool to locally deliver NO *in vitro*, directly to the target site of application. The results of this study highlighted the promising use of S-nitrosated iron oxide magnetic nanoparticles as a new approach in cancer therapy.

2. MATERIALS AND METHODS

2.1. Materials. Mercaptosuccinic acid (MSA), dimercaptosuccinic acid (DMSA), sodium nitrite (NaNO₂), iron(III) chloride hexahydrate (FeCl₃·6H₂O), iron(II) chloride tetrahydrate, ammonium hydroxide (NH₄Cl), oleic acid, toluene, dimethylsulfoxide (DMSO), 5',5-dithiobis(2-nitrobenzoic acid) (DTNB), phosphate buffered saline (PBS), pH 7.4, ethylenediaminetetraacetic acid (Sigma-Aldrich Ch. Co., Inc., USA), and hydrochloric acid (12 mol/L, Synth, USA) were used as received. Aqueous solutions were prepared using analytical grade water from a Millipore Milli-Q Gradient filtration system. Cell culture experiments were performed with DMEM, MacCoy's, and RPMI media (Gibco) in the presence of 10% fetal calf serum (Gibco), supplemented with 1% antibiotics.

2.2. Synthesis of Iron Oxide (Fe₃O₄) Magnetic Nanoparticles Coated with Thiol Groups: MSA-Fe₃O₄ or DMSA-Fe₃O₄. Fe₃O₄ nanoparticles were synthesized in an acidic medium by the coprecipitation technique, as previously described.²⁶ A volume of 4.0 mL of FeCl₂·4H₂O (1.0 mol/L) and a volume of 8.0 mL of FeCl₃·6H₂O (0.5 mol/L), prepared in 1.0 mol/L HCl, were mixed and strongly stirred, whereas 50.0 mL of NH₄Cl (0.7 mol/L) was gradually dropped into the previously described solution. The addition of bases resulted in the formation of a black precipitate. This precipitate was magnetically decanted, followed by the addition of 6.0 mL of oleic acid. This mixture was then stirred for 20 min. The solution was decanted and washed several times with ethanol, leading to the formation of Fe₃O₄ nanoparticles covered with oleic acid.

Oleic acid coated-Fe₃O₄ (50 mg) were suspended in 5.0 mL of toluene and mixed with 2.0 g of MSA or DMSA dissolved in dimethylsulfoxide (DMSO). This final mixture was stirred for 14 h, and a black precipitate was formed and isolated by magnetic decantation. The black powder was washed several times with ethanol. This procedure led to the preparation of Fe₃O₄ nanoparticles coated with MSA (MSA-Fe₃O₄) or with DMSA (DMSA-Fe₃O₄). Both nanoparticles are thiolated-Fe₃O₄ nanoparticles.

2.3. Characterization of Thiolated-Fe₃O₄ Nanoparticles.

2.3.1. X-ray Diffraction (XRD). The diffractograms were obtained with approximately 200 mg of powdered MSA-Fe₃O₄ or DMSA-Fe₃O₄ placed onto a glass substrate of 2 × 2 cm². The measurements were performed in reflection setup, with a conventional X-ray generator (CuK α radiation of 1.5418 Å and a graphite monochromator) coupled to a scintillation detector. The angular scanning performed on all samples ranged from 10 to 70° with 0.05° step-width at 5 s per angle.

2.3.2. Scanning Electron Microscopy (SEM) and Energy Dispersive X-ray Fluorescence Spectrometry (EDS). Particle morphology was characterized by scanning electron microscopy (Jeol JSM T-300 electron microscope Tokyo, Japan) at a voltage of 20 kV, with an energy-dispersive X-ray spectrometry (EDS) system. The EDS technique was used to map the distribution of sulfur, iron, and oxygen atoms on the nanoparticles.

2.3.3. Vibrating Sample Magnetometry (VSM). The magnetic curves of the thiolated Fe₃O₄ nanoparticles were calculated at room temperature, and the apparatus was calibrated to a Ni pattern. The magnetization measurements were carried out on a known quantity of powdered sample, which was slightly pressed and conditioned in cylindrical Lucite holders.

2.3.4. Hydrodynamic Size and Size Distribution of Thiolated Nanoparticles. The hydrodynamic diameter and polydispersity index (PDI) of thiolated Fe₃O₄ nanoparticles were measured by photon correlation spectroscopy (PCS) (Nano ZS Zetasizer, Malvern Instruments Corp.) at 25 °C in polystyrene cuvettes, with a path length of 10 mm. The standard report for size measurement was intensity. The dispersion of the MSA-Fe₃O₄ nanoparticles was centrifuged and diluted into a solution of 0.1 mmol L⁻¹ potassium chloride prior to analysis. The measurements were performed in triplicate with the standard error of the mean.

2.3.5. Determination of the Amount of Thiol Groups on the Surface of MSA- or DMSA-Fe₃O₄ Nanoparticles. The number of thiol groups (–SH) on the surface of MSA- or DMSA-Fe₃O₄ nanoparticles was measured by the DTNB reaction, based on the absorbance at 412 nm ($\epsilon = 14,150 \text{ mol L}^{-1}\text{cm}^{-1}$) of the 2-nitro-5-thiobenzoate anion

(TNB²⁻) generated in the reaction of -SH groups with DTNB, as previously reported.³² Appropriate amounts of thiolated nanoparticles were added to 3.0 mL of 0.01 mol L⁻¹ DTNB in PBS buffer (pH 7.4) containing 1 mmol L⁻¹ of ethylenediaminetetraacetic acid. After 5 min of incubation, the suspensions were filtered by centrifugal ultrafiltration using a Microcon centrifugal filter device containing ultrafiltration membranes (MWCO 10-kDa molar mass cutoff filter, Millipore, Billerica, MA, USA). The supernatant was placed into a quartz cuvette, and the intensity of the absorption band at 412 nm was measured in an UV-vis spectrophotometer (Agilent, model 8553, Palo Alto, CA, USA). The experiments were performed in triplicate.

2.4. Nitrosation of the Thiol Groups of Thiolated Fe₃O₄ Nanoparticles. The thiol groups on the surface of MSA- or DMSA-Fe₃O₄ were nitrosated, leading to the formation of NO-releasing nanoparticles, as previously described.²⁶ In this step, filtered MSA- or DMSA-MNPs (1.0 mg/mL) were suspended in deionized water. A volume of 200 μL of aqueous sodium nitrite (60 mmol/L) was added to MSA- or DMSA-Fe₃O₄ nanoparticles. Molar excess of nitrite in relation to the amount of thiol groups on the surface of MSA- or DMSA-nanoparticles was used. After 30 min of incubation, the nanoparticle suspension was filtered by centrifugal ultrafiltration using a Microcon centrifugal filter device containing ultrafiltration membranes (MWCO 10-kDa molar mass cutoff filter, Millipore, Billerica, MA, USA) and washed three times with deionized water to remove excess unreacted nitrite. This procedure led to the preparation of S-nitroso-MSA or S-nitroso-DMSA Fe₃O₄ magnetic nanoparticles.²⁶

2.5. In Vitro Experiments. **2.5.1. Cell Descriptions.** For the analyses involving lymphocytes, the cells were separated from whole blood using Ficoll-Paque PLUS medium (GE Healthcare, Little Chalfont, UK). The blood was provided by donors aged between 18 and 24 years (with signed terms of agreement forms). The project was approved by the Ethics Committee of the Sorocaba University (protocol #121.696). Blood samples were collected throughout the procedure using disposable materials. The lymphocytes were placed in Roswell Park Memorial Institute (RPMI) 1600 culture medium (Gibco) containing 300 μg/mL of L-glutamine and 200 μg/mL of NaHC3 supplemented with 5% bovine fetal serum, 50 μg/mL of gentamicin sulfate (antibiotic), and 2 μg/mL of amphotericin B (antifungal). The culture was kept at 37 °C in a humidified atmosphere containing 5% CO₂. The 3T3 cell mouse fibroblasts were provided by a bank of the Cell Bank of Rio de Janeiro

(APABCAM, Brazil), and the MCF-7 line (breast cancer cells) was provided by the Biomembrane Laboratory of the State University of Campinas (UNICAMP, Brazil). The Chinese hamster ovary (CHO) cells (ovary *Cricetulus griseus*, hamster, Chinese) were provided by the MAX Rubens Institute. The cells were kept at 37 °C in a humid atmosphere with 5% CO₂ in Dulbecco's modified Eagle's medium (DMEM) containing 584 μg/mL of L-glutamine and 370 μg/mL of NaHCO₃ supplemented with 10% bovine fetal serum, 50 μg/mL of gentamicin sulfate, and 2 μg/mL of amphotericin B. Aliquots, each containing approximately 106 cells per mL, were cryopreserved in nitrogen in bovine fetal serum with 10% dimethyl sulfoxide. For each new experiment, a fresh aliquot was withdrawn, washed, and plated out.

2.5.2. Incubation Cells with Thiolated and S-Nitrosated Fe₃O₄ Nanoparticles. The cells (human lymphocytes, 3T3 fibroblasts, CHO, and MCF-7 breast cancer cells) were incubated with thiolated nanoparticles (MSA- or DMSA-Fe₃O₄) and S-nitrosated nanoparticles (S-nitroso-MSA or S-nitroso-DMSA Fe₃O₄) at the following nanoparticle concentrations: 0.01; 0.1; and 0.5 mg/mL, for 1 or 24 h. Negative and positive controls received PBS and H₂O₂ (200 μmol/L), respectively. The cytotoxicity and genotoxicity of the cells upon their incubation with nanoparticles were evaluated as described below.

2.5.3. Tali Analysis. Cell viability was measured using a Tali apoptosis kit consisting of Annexin V Alexa Fluor 488, propidium iodide (Invitrogen), and a Tali image-based cytometer, which enabled the numbers of viable, apoptotic, and dead cells to be counted. The Tali image-based cytometer is based on the images of the cells and their interactions with the reagents Annexin V Alexa Fluor 488 (which has affinity for phosphatidyl serine) and propidium iodide (which has affinity for DNA), making it possible to distinguish the percentage of viable cells, apoptotic cells, and necrotic cells. The cells that had been treated with thiolated or S-nitrosated Fe₃O₄ at nanoparticle concentrations (0.01; 0.1 and 0.5 mg/mL) were centrifuged and concentrated to 1 × 10⁶ cells per mL. Aliquots of 100 μL of the sample were prepared according to the specifications of the kit, and the tests were performed in triplicate. Relative indexes of necrosis and apoptosis of the treated groups (thiolated or S-nitrosated nanoparticles) were measured by considering the ratio of the values of necrosis and apoptosis of the treated groups related to the negative control group, according to the following equations:

$$\text{Relative necrosis index} = (\text{number of necrotic cells in the treated group}) / (\text{number of necrotic cells in the negative control group}) \quad (1)$$

$$\text{Relative apoptosis index} = (\text{number of apoptotic cells in the treated group}) / (\text{number of apoptotic cells in the negative control group}) \quad (2)$$

2.5.4. Comet Assay. Each treatment group involved 10 μL of cells (human lymphocytes, 3T3 fibroblasts, and MCF-7 breast cancer cells) in 110 μL of low melting point agarose (0.6%), and the mixtures were placed onto microscope slides that had been precoated with normal melting point agarose (1.5%). Coverslips were positioned over the materials, and the slides were placed in a refrigerator for polymerization. After polymerization, the coverslips were removed, and the slides were treated for 60 min with an ice-cold (4 °C) lysis solution (2.5 mol/L NaCl, 0.1 mol/L ethylenediaminetetraacetic acid (EDTA), 10 mmol/L tris(hydroxymethyl)aminomethane (Tris), and 1% Triton X-100TM, pH 10). All of the groups were incubated in an electrophoresis buffer (0.3 mol/L NaOH and 1 mM mol/L EDTA, pH 13) for 20 min, followed by electrophoresis for 20 min at 1.3 V/cm. After electrophoresis, the slides were covered with a neutralizing solution (0.4 mol/L Tris, pH 7.5) for 5 min, washed three times with distilled water, and allowed to rest overnight at room temperature. Prior to staining, the dry slides were left in a fixing solution (15% w/v trichloroacetic acid, 5% (w/v) zinc sulfate, and 5% glycerol) for 10

min, after which they were further washed three times with distilled water. After these procedures, the slides were allowed to rest at room temperature for 1.5 h. They were then rehydrated with distilled water and stained for approximately 15 min with silver staining solution consisting of solution A (0.2% w/v ammonium nitrate, 0.2% w/v silver nitrate, 0.5% w/v tungstosilicic acid, 0.15% v/v formaldehyde, and 5% w/v sodium carbonate) and solution B (5% sodium carbonate) (34:66 v/v). Next, they were bathed in distilled water and then in stop solution. Finally, the slides were again washed with distilled water and allowed to dry at room temperature. Staining using silver is analogous to fluorescence, during which the positive charge of the silver enables it to bind with DNA and DNA fragments, producing the characteristic color. Throughout the procedures involving cellular material, both natural light and light from the fluorescent lamps were avoided to prevent their possible influencing of the results.

Analyses were performed using the Zeiss Axiovert optical microscope, and at least 100 cells were counted on each slide, with 3 slides for each test (approximately 300 cells). The experiment was performed

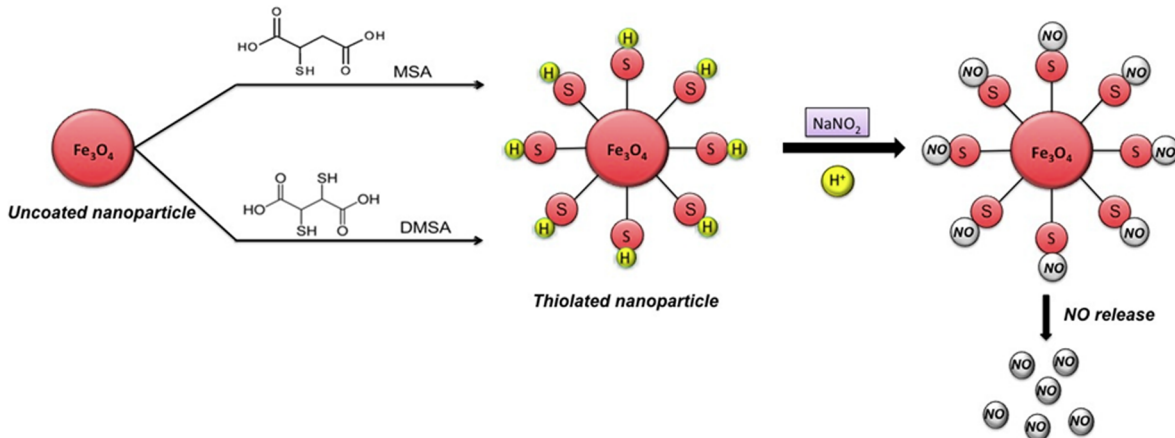


Figure 1. Schematic representation of the formation of thiolated Fe_3O_4 nanoparticles coated with mercaptosuccinic acid (MSA) or dimercaptosuccinic acid (DMSA). Thiolated nanoparticles were nitrosated upon incubation with sodium nitrite in aqueous solution, leading to the formation of S-nitroso- Fe_3O_4 nanoparticles (S-nitroso-MSA or S-nitroso-DMSA- Fe_3O_4 nanoparticles), which are spontaneous NO donors.

in triplicate, totaling 900 cells for analysis from each sample tested. The comet assay analyses were performed by assigning a score of 0 to 4, according to the quantity of DNA in the tail and the length of the tail as follows: score 0 corresponded to intact cells; score 1, to cells with minimal damage; score 2, to those with average damage; score 3, to those with severe damage; and score 4, to those with maximum damage.³⁶ For this visual method, the number of cells found for each score was multiplied by the value of the score; all of the values were summed at the end of the analysis of each slide. Because the score depended on the number of cells observed, an index of tail damage (TD) was created by dividing the score given to the slide by the number of cells analyzed on the slide.

2.5.5. Influence of a Magnetic Field on Killing MCF-7 and CHO Cells upon Incubation with S-Nitroso-Magnetic Nanoparticles. CHO and MCF-7 cell suspensions ($2 \times 10^5 \text{ mL}^{-1}$) were poured into culture bottles (25 cm^2). After the cell adherence, only half of the bottles were submitted to a magnetic field. The cells were then incubated with S-nitroso-MSA- Fe_3O_4 (0.1 mg/mL) for 24 h to evaluate the influence of the magnetic field on the suspension and consequent viability of the exposed cells. After the incubation period, the cultures were washed, fixed with methanol/acetic acid (7:1) and colored with Giemsa. The visualization was performed by optical microscopy (Zais-Axovert 60). Dead cells were assumed to be washed out.

3. RESULTS AND DISCUSSION

3.1. Characterization of Thiolated Fe_3O_4 Nanoparticles. In this work, Fe_3O_4 nanoparticles were successfully synthesized by the coprecipitation method, as previously described.²⁶ The nanoparticles were coated with two small thiol-containing ligands, MSA or DMSA. MSA contains one sulphydryl group per molecule, while DMSA contains two sulphydryl groups per molecule. Thiolated Fe_3O_4 nanoparticles were characterized and nitrosated, leading to the formation of NO-releasing nanoparticles. Figure 1 shows the schematic representation of the thiolation of Fe_3O_4 nanoparticles, followed by their nitrosation, which led to the formation of S-nitroso- Fe_3O_4 , a spontaneous NO donor.²⁶

Figure 2 shows a representative X-ray diffractogram of solid thiolated Fe_3O_4 nanoparticles coated with MSA. The diffraction pattern (indicated in Figure 2) confirms that the crystallographic structure of the nanoparticle corresponded to magnetite (Fe_3O_4) (JCPDS 20–596). As previously described, crystallite sizes in the range of 10–15 nm were obtained by taking into account the (311) Bragg's reflection.²⁶

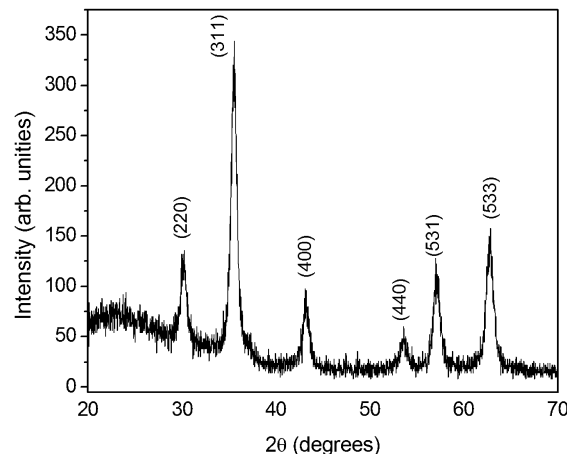


Figure 2. X-ray powder diffraction from a representative sample of a thiolated Fe_3O_4 nanoparticle coated with MSA, displaying the Bragg peak reflections of magnetite.

Figure 3A shows the SEM image of the MSA- Fe_3O_4 nanoparticles. It can be observed that the nanoparticles have a spherical shape. The composition of thiolated Fe_3O_4 nanoparticles was examined by EDS. Figure 3B shows the EDS spectra of the MSA-coated nanoparticles, which indicated the presence of an energy-dispersive X-ray emission of iron (Fe), oxygen (O), and sulfur (S) atoms, as expected. The weighted percentages of Fe, O, and S were found to be 51.13; 44.42; and 4.45%, respectively. Figure 3C shows the SEM image of MSA- Fe_3O_4 , with the red dots representing the EDS elemental mapping of Fe atoms. As expected, Fe atoms are homogeneously dispersed on the nanoparticles. Similarly, Figure 3D shows the SEM image of a MSA- Fe_3O_4 nanoparticle, with the red and yellow dots representing the EDS elemental mapping of Fe and S atoms, respectively. A homogeneous distribution of dots in the islands of sulfur atoms can be observed in the mapped area. Taken together, these results confirm the formation of spherical and well-dispersed thiolated Fe_3O_4 nanoparticles as well as the presence of a homogeneous MSA coating on the surface of the nanoparticles.

Magnetization analyses were carried out using isothermal magnetic measurements at room temperature under an applied field. As can be observed in Figure 4, the hysteresis loops show

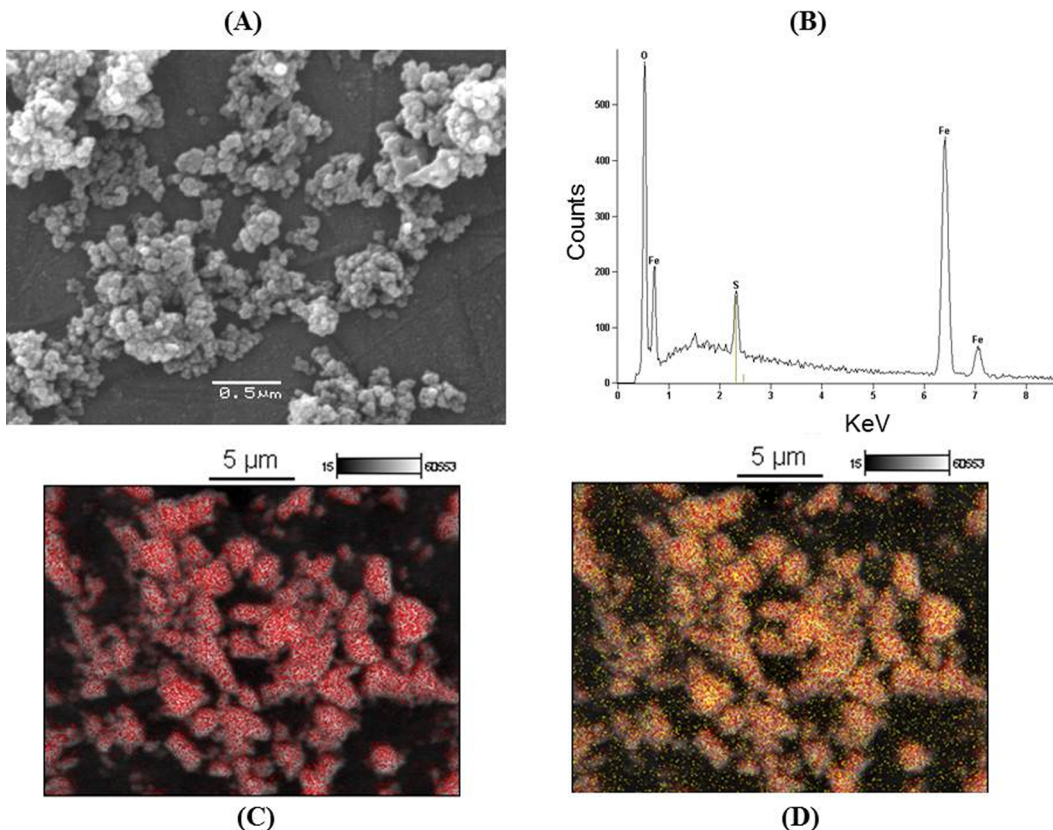


Figure 3. Morphological characterizations of thiolated Fe_3O_4 nanoparticles coated with MSA: (A) Scanning electron microscopy image; (B) elemental analysis showing EDS peaks of iron (Fe), oxygen (O), and sulfur (S) atoms. The sulfur peak is due to the surface $-\text{SH}$ groups of the MSA- Fe_3O_4 nanoparticle; (C) scanning electron microscopy image in which red dots corresponds to iron (Fe) atoms; (D) scanning electron microscopy image in which red dots correspond to iron (Fe) atoms and yellow dots to sulfur (S) atoms.

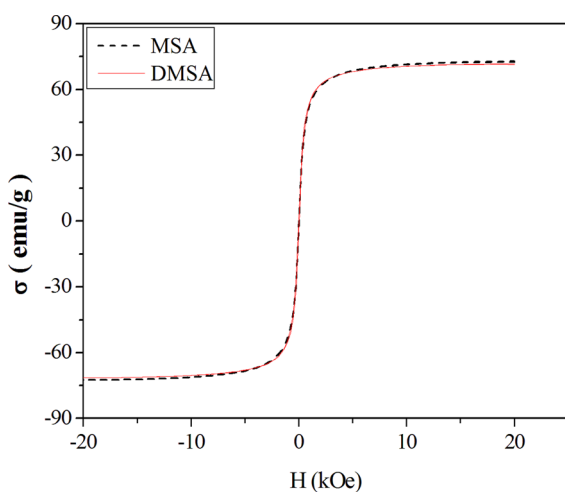


Figure 4. Magnetization curves at room temperature for MSA- or DMSA-coated Fe_3O_4 nanoparticles, as indicated in the Figure.

that the thiolated Fe_3O_4 nanoparticles have superparamagnetic behavior at room temperature. This property is highly important for the biomedical application of NO-releasing magnetic nanoparticles. Once injected in the blood, these nanoparticles can be guided to the target site (such as a tumor area) under an external magnetic field. This means that superparamagnetic Fe_3O_4 nanoparticles can deliver the active compound (such as NO) directly to the intended site of

application. This property makes Fe_3O_4 nanoparticles an interesting vehicle for directly targeted biomedical applications.

The average hydrodynamic diameter and polydispersity index (PDI) of MSA- Fe_3O_4 nanoparticles were found to be 226 ± 19 nm and 0.30 ± 0.01 , respectively. These results indicate that thiolated nanoparticles have a hydrodynamic diameter in the nanoscale and a low polydispersity index, indicating an excellent dispersion in water, which makes these nanoparticles an attractive vehicle for drug delivery in biomedical applications.

The amounts of free thiol ($-\text{SH}$) groups on the surface of MSA- or DMSA- Fe_3O_4 were determined by the reaction of the thiolated nanoparticles with a thiol-specific reagent, DTNB.³² Values of $40 \pm 7 \mu\text{mol SH/g}$ of MSA- Fe_3O_4 and $105 \pm 8 \mu\text{mol SH/g}$ of DMSA- Fe_3O_4 nanoparticles were found.

3.2. Nitrosation of Thiolated Fe_3O_4 Nanoparticles Leading to NO-Releasing Nanoparticles. Free thiol (SH) groups on the surface of MSA- or DMSA- Fe_3O_4 were nitrosated by the addition of sodium nitrite leading to the formation of S-nitroso-MSA or S-nitroso-DMSA- Fe_3O_4 nanoparticles (Figure 1). Nitrite (NO_2^-) is in equilibrium with nitrous acid (HNO_2) in acidified aqueous solution. HNO_2 is assigned as the nitrosating agent of SH groups to cause the formation of $-\text{SNO}$ groups on the nanoparticle's surface.^{26,37} As molar excess of nitrite was added to thiolated nanoparticles, completed S-nitrosation of the nanoparticles can be assumed (which corresponds to $40 \pm 7 \mu\text{mol SNO/g}$ of MSA- Fe_3O_4 and $105 \pm 8 \mu\text{mol SNO/g}$ of DMSA- Fe_3O_4 nanoparticle). Thus, the amounts of free thiol groups on the surface of MSA- or

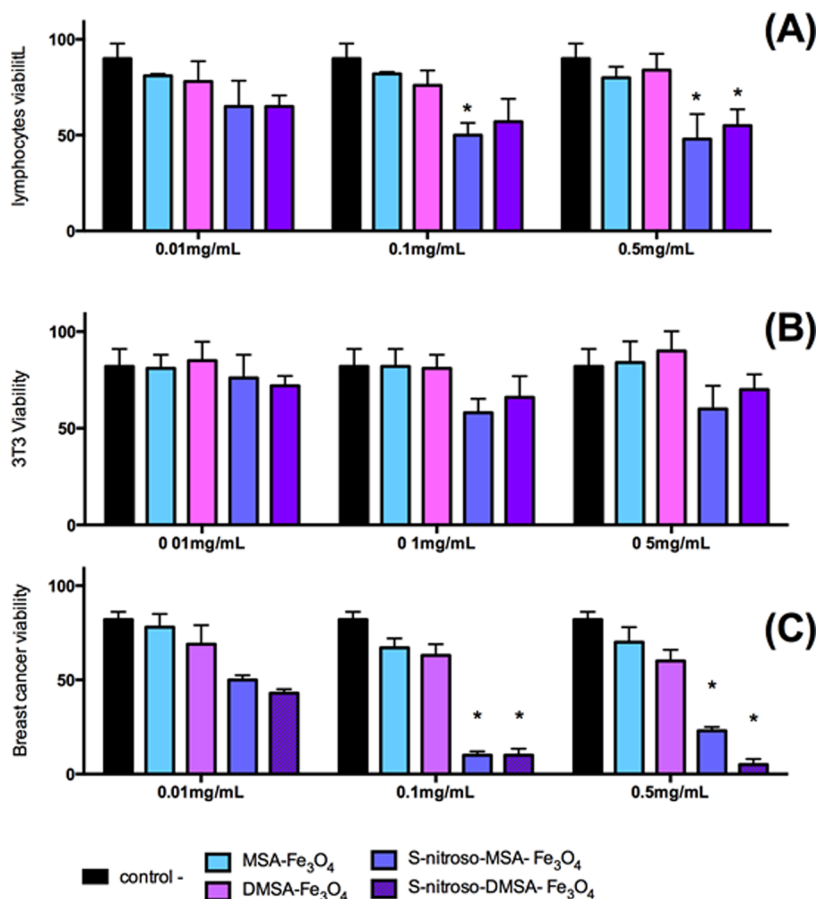


Figure 5. Cell viability of human lymphocytes (panel A), 3T3 cell mouse fibroblasts (panel B), and breast cancer (MCF-7) (panel C) cells treated with thiolated nanoparticles (MSA- or DMSA-Fe₃O₄) and NO-releasing nanoparticles (S-nitroso-MSA or S-nitroso-DMSA-Fe₃O₄) at different concentrations, as indicated in the Figure. Incubation time: 1 h. Negative controls employed phosphate buffered saline (PBS). Notes: *, significant alterations compared with the control (analysis of variance, $P < 0.05$). Values are expressed as the means of three experiments ($n = 3$).

DMSA-nanoparticles can be considered sufficient for loading high amounts of NO on the nanoparticle surfaces, once the extent of S-nitrosation performed in the nanoparticles display high toxic effects on healthy and tumor cell lines (sections 3.3–3.5).

S-Nitrosothiols (-SNO groups) are spontaneous NO carriers and donors³⁸ due to the S-NO homolytic bond cleavage (S–N) with the release of free NO (as indicated in Figure 1). As previously reported, S-nitroso-MSA-Fe₃O₄ magnetic nanoparticles are able to spontaneously release NO for several hours, and the amount of NO released is in the micromolar range.²⁶ Indeed, micromolar amounts of NO are required for anticancer therapies.^{33,39,40} The subproducts of NO that are released from S-nitrosated nanoparticles are the dimmers of MSA or DMSA, as bound by a sulfur bridge.²⁶ Both the thiolated nanoparticles and S-nitroso-Fe₃O₄ nanoparticles were incubated with different cells for their *in vitro* toxicological evaluations, as described below.

3.3. Cell Viability, Apoptosis, and Cell Death. Cell viability studies were performed by treating 3T3 cell mouse fibroblasts (Figure 5A), human lymphocytes (Figure 5B), and MCF-7 breast cancer cells (Figure 5C) with thiolated nanoparticles (MSA- or DMSA-Fe₃O₄) and NO-releasing nanoparticles (S-nitroso-MSA or S-nitroso-DMSA-Fe₃O₄) at different concentrations. It was observed that the thiolated nanoparticles (MSA- or DMSA-Fe₃O₄) did not significantly decrease the cell viability of either 3T3 or lymphocytes

compared to the control group (cells treated with PBS). Figure 5A shows that S-nitroso nanoparticles (S-nitroso-MSA or S-nitroso-DMSA-Fe₃O₄) at the lowest tested concentration (0.01 mg/mL) did not reduce the cell viability of 3T3 cells. However, at higher S-nitrosated nanoparticle concentrations (0.1 and 0.5 mg/mL), a decrease in 3T3 viability was observed either for S-nitroso-MSA or S-nitroso-DMSA-Fe₃O₄ particles (Figure 5A). Similarly, Figure 5B shows that S-nitrosated nanoparticles did not decrease human lymphocyte viability at the lowest tested concentration. By increasing the S-nitrosated-Fe₃O₄ nanoparticle concentrations (0.1 and 0.5 mg/mL), a statistically significant decrease in lymphocyte viability was observed (Figure 5B). Moreover, human lymphocytes were found to be more susceptible to S-nitroso nanoparticles in comparison with 3T3 cells. Figure 5C shows that thiolated nanoparticles (MSA- or DMSA-Fe₃O₄) caused a slight decrease in cell viability compared to that of the control group. However, S-nitroso-MSA and S-nitroso-DMSA Fe₃O₄ greatly reduced MCF-7 cell viability, mainly at the higher tested concentrations (0.1 and 0.5 mg/mL).

Figure 5 shows that breast cancer cells (MCF-7) presented a higher susceptibility to S-nitrosated Fe₃O₄ particles than the other cells analyzed (3T3 and lymphocytes). Taken together, these results indicate that S-nitrosated Fe₃O₄ nanoparticles may have relevant applications for the treatment of cancer cells.

The low toxicity shown by the cells submitted to the vehicle (thiolated-Fe₃O₄) is very important. As previously reported,

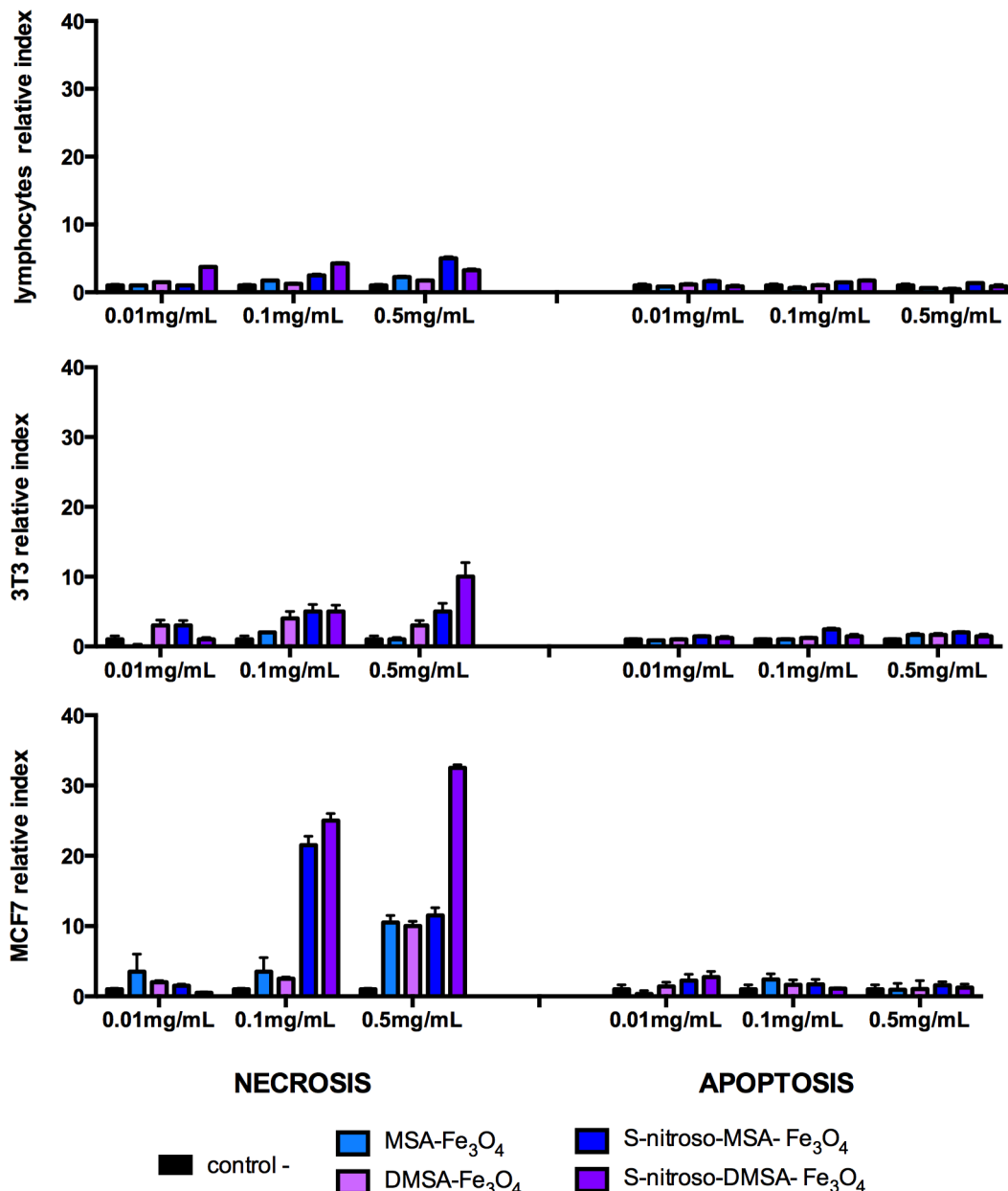


Figure 6. Relative indexes of cell necrosis and apoptosis in human lymphocytes (panel A), 3T3 cells (panel B) and MCF-7 breast cancer cells (panel C) treated with thiolated nanoparticles (MSA- or DMSA- Fe_3O_4) and NO-releasing nanoparticles (S-nitroso-MSA or S-nitroso-DMSA- Fe_3O_4) at different concentrations, as indicated in the Figure. Incubation time: 1 h. Negative controls employed PBS. Values are expressed as the means of three experiments ($n = 3$).

thiolated nanoparticles, such as DMSA-coated maghemite nanoparticles, resulted in weak cytotoxic and genotoxic effects.¹³ The lack of toxic effects observed for the thiolated iron-based nanoparticles is attributed to the presence of the small thiol-containing molecules, such as MSA or DMSA, adsorbed onto the nanoparticle's surface, which acts as a barrier to direct contact between the nanoparticle and the exposed cells, avoiding potential toxic effects. In contrast, the observed toxic effect can be assigned to the presence of S-NO groups on the surface of the nanoparticles. The chemical nature of the nanoparticle coating seems to imply different cell responses in terms of cytotoxicity. Recently, the cytotoxic effects of DMSA- Fe_2O_3 nanoparticles were evaluated using cultured human aortic endothelial cells (HAECs).²¹ The authors observed a dose-dependent cytotoxicity of DMSA- Fe_2O_3 on HAECs, and

concentrations less than 0.02 mg/mL had limited toxic effects.²¹

It is reasonable to suppose that S-nitrosated Fe_3O_4 magnetic nanoparticles would be an interesting drug delivery system for fighting cancer, in particular breast cancer cells, without any loss of particle magnetization. In the case of breast cancer treatment, unfortunately, side effects, including cardiovascular disorders, have been reported among long-term cancer survivors treated with chemotherapeutic drugs, such as tamoxifen citrate, capecitabine, and epirubicin.⁹ In this context, breast cancer cells were incubated with S-nitroso nanoparticles to explore a potent new treatment approach.

Figure 6 shows the indexes of cell death and apoptotic cells for human lymphocytes (Figure 6A), 3T3 cells (Figure 6B), and MCF-7 cells (Figure 6C) after 1 h of exposure to thiolated

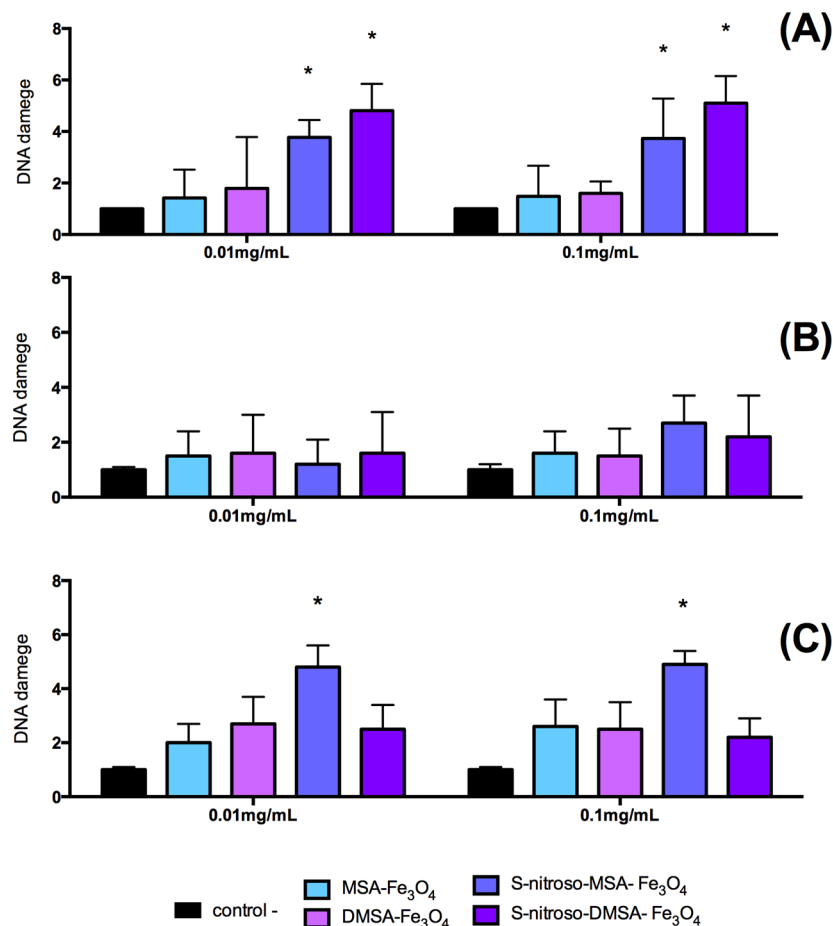


Figure 7. Results of the tail damage obtained for lymphocytes (panel A), 3T3 cells (panel B), and breast cancer cells (MCF-7) (panel C) after treatments with the thiolated nanoparticles (MSA- or DMSA-Fe₃O₄) and NO-releasing nanoparticles (S-nitroso-MSA or S-nitroso-DMSA-Fe₃O₄) at 0.01 and 0.1 mg/mL, respectively, as indicated in the Figure. Incubation time: 1 h. Negative controls employed PBS. Notes: *, significant alterations compared with the control (analysis of variance, $P < 0.05$). Values are expressed as the means of three experiments ($n = 3$).

and S-nitrosated particles at 0.01, 0.1, and 0.5 mg/mL, as indicated. The levels of apoptosis for lymphocytes incubated either with thiolated or S-nitrosated nanoparticles were observed to be similar to those in the negative control group. Thiolated nanoparticles led to a slight increase in cell death in a concentration-dependent manner (Figure 6A).

For 3T3 cells, the levels of apoptosis for all particles (thiolated and S-nitrosated) at all tested concentrations were observed to be similar to those of the negative control group (Figure 6B). The thiolated nanoparticles showed a slight increase in the number of dead cells, in comparison with that of negative controls, mainly DMSA-Fe₃O₄ nanoparticles (Figure 6B); however, the results were not significantly different. For S-nitrosated nanoparticles, curiously, S-nitroso-MSA did not significantly increase the number of dead cells. In contrast, S-nitroso-DMSA significantly increased the number of 3T3 cell death in a concentration dependent manner (Figure 6B).

In parallel, Figure 6C shows the results for the MCF-7 breast cancer cell line. Low indexes of apoptosis were observed for both thiolated and S-nitrosated nanoparticles in all tested concentrations. However, S-nitrosated Fe₃O₄ nanoparticles greatly increased cell death at 0.1 and 0.5 nanoparticle concentrations (Figure 6C), highlighting the toxic effects of these nanoparticles toward breast cancer cells.

Taken together, these results indicate that MSA- and DMSA-Fe₃O₄ nanoparticles did not significantly induce cell death or

apoptosis for all cell lines, in comparison with the negative controls. These results are in accordance with the viability results of cells after exposure to thiolated nanoparticles (Figure 5). As expected, the thiolated nanoparticles did not decrease cell viability or induce cell death/apoptosis. In contrast, S-nitrosated nanoparticles decreased cell viability mainly by cell death (necrosis) rather than by apoptosis. NO directly inhibits the activity of caspases, proving itself an efficient means of blocking apoptosis.³³ Indeed, the main antiapoptotic effect of NO is associated with the inhibition of caspases by the S-nitrosation of redox-sensitive thiol in the enzyme's catalytic site.⁴¹

The sustained generation of high levels of NO has been shown to result in cytotoxicity and necrotic cell death.⁴¹ NO can destroy cells via necrosis by disrupting cell membranes and organelles.⁴² The toxicity of NO toward different cell lines is attributed to oxidative and nitrosative stress, protein modification, mitochondrial dysfunction, damage to the DNA, and disruption of the energetic metabolism. As a consequence, these disturbances can lead to cell death by necrosis or apoptosis, depending on the severity of the damage.^{41,43}

As an extremely versatile messenger in biological media, NO is implicated in a number of different pathological and physiological functions.⁴⁴ In fact, the ATP depletion caused by NO stimulates the production of superoxide (O₂^{•-}) by the respiratory chain in mitochondria. NO is known to react with

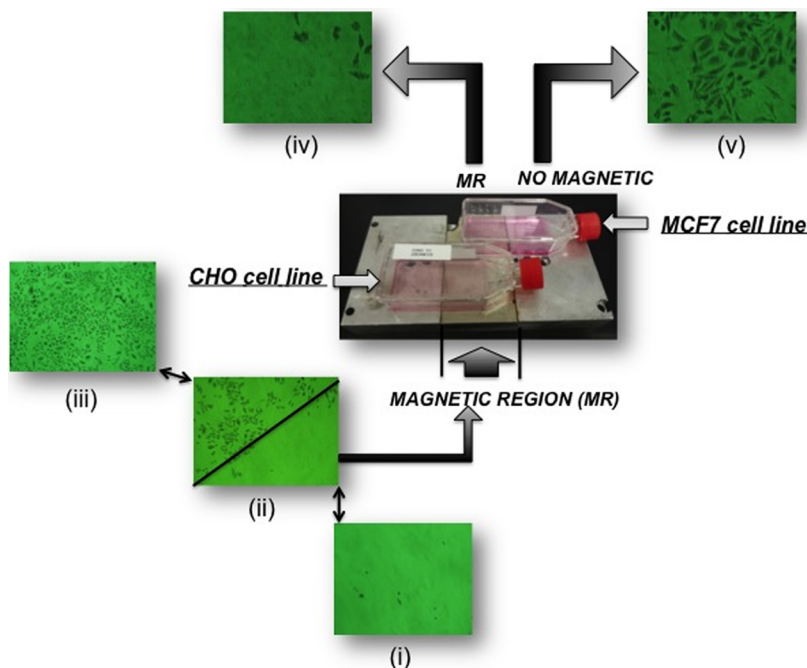


Figure 8. Representative optical microscopy images of Chinese hamster ovary (CHO) cells (i, ii, and iii) and MCF-7 cancer cells (iv and v) treated with S-nitroso-MSA (0.1 mg/mL) for 1 h, with and without the influence of the external magnetic field (MR = magnetic region), as represented in the Figure. Optical images of the following: (i) region of the well dishes in which CHO cells were under the influence of the magnet field; (ii) in the lower section of the image, cells (CHO) were under the influence of the magnetic field, whereas, in the upper part of the image, cells (CHO) were not under the influence of the magnetic field; the trace represents the separation of the magnetic field; (iii) region of the well dishes in which CHO cells were free from the influence of the magnetic field; and (iv) region of the well dishes in which MCF-7 cells were under the influence of the external magnetic field.

superoxide, leading to the formation of harmful peroxynitrite (ONOO^-), according to eq 3.



Peroxynitrite-mediated pathways are thus important to NO-induced cell death.⁴³ Peroxynitrite can S-nitrosate and precipitate the tyrosine nitration of important biomolecules, such as proteins, leading to a change in their function.⁴⁵ Thus, peroxynitrite can cause lipid peroxydation, DNA cleavage, and tyrosine nitration.^{33,44} It should be noted that MCF-7 cells showed higher susceptibility to S-nitrosated nanoparticles in comparison with that of human lymphocytes and 3T3 cells (Figure 5). This result may be understood by considering that cancer is closely related to oxidative stress, in which the production of reactive oxygen species, such as the superoxide radical, is elevated in comparison to that in normal conditions. As NO readily reacts with superoxide forming peroxynitrite (eq 3), the higher susceptibility of MCF-7 toward S-nitrosated nanoparticles may be related to the accelerated production of reactive nitrogen/oxygen species, such as peroxynitrite.^{41–45} In this context, NO is able to finely regulate cell death, either under physiological conditions or pathological ones, such as cancer and susceptibility to cancer therapies.⁴⁴

3.4. DNA Damage. In this work, the genotoxic effects of thiolated and S-nitrosated Fe_3O_4 nanoparticles in healthy and cancer cells were assessed by the comet assay, which detects DNA strand breaks following either direct damage induced by the nanoparticles or indirect damaging effects linked to the DNA repair process. Indeed, the comet assay is able to quantitatively detect the DNA damage caused by alkylating or oxidizing agents and intercalating.^{36,46}

Figure 7 represents the genotoxic effects (DNA damage) of human lymphocytes (7A), 3T3 cells (7B), and MCF-7 cells (7C) incubated with thiolated nanoparticles (MSA- and DMSA- Fe_3O_4 nanoparticles) and S-nitrosated nanoparticles (S-nitroso-MSA and S-nitroso-DMSA- Fe_3O_4) at 0.01 and 0.1 mg/mL, respectively. For human lymphocytes and 3T3 cell lines, thiolated nanoparticles showed no significant genotoxic effects at the two tested nanoparticle concentrations. This result is in accordance with the lack of cytotoxic effects observed for thiolated nanoparticles (Figure 5). Figure 7A reveals that S-nitroso-MSA or S-nitroso-DMSA nanoparticles result in significant genotoxic effects on the lymphocyte cells at both tested concentrations. In addition, the DNA damage of S-nitrosated particles at both concentrations was not observed to have significant genotoxicity regarding 3T3 cells (Figure 8B).

These results indicate that human lymphocytes were more sensitive to treatment with S-nitroso-MSA and S-nitroso-DMSA- Fe_3O_4 than 3T3 cells (Figures 5 and 8). Although NO is a simple diatomic molecule, the complexity of its redox chemistry in biological systems may account for its diverse biological functions.

As can also be observed in Figure 7C, the DNA damage of MCF-7 cancer cells incubated with thiolated Fe_3O_4 at 0.01 and 0.1 mg/mL, respectively, showed that MSA- or DMSA- Fe_3O_4 can have slight genotoxic effects toward breast cancer cells. Curiously, S-nitroso-DMSA did not cause significant DNA damage to MCF-7 cancer cells, although these nanoparticles were found to have cytotoxic activities (Figure 5C). In contrast, S-nitroso-MSA Fe_3O_4 nanoparticles showed a great increase in DNA damage, in comparison with that of the control group (Figure 7C).

Taken together, these results indicate that S-nitrosated nanoparticles have genotoxic effects in different cell lines, while thiolated nanoparticles have few genotoxic effects. The cytotoxic effects caused by NO and peroxynitrite in tumor cells have been shown to result from DNA damage.⁴¹ NO participates in genotoxic events mainly by causing DNA lesions through the formation of toxic and mutagenic reactive nitrogen species via the direct modification of DNA structure or the impairment of the DNA repair process.³³ It has been reported that the DNA damage caused by NO may occur via deamination, oxidation, and/or strand breakage.⁴⁷

3.5. Influence of a Magnetic Field on the Viability of CHO and MCF-7 Cells upon Incubation with S-Nitroso-Magnetic Nanoparticles. Using *in vivo* systemic administration (i.e., intravenous), functionalized iron oxide magnetic nanoparticles, such as S-nitrosated Fe₃O₄, can be guided to the target tissues/organs (e.g., tumor), producing local cytotoxic and genotoxic effects. Hence, pharmaceutical drugs can be loaded onto the surface of the magnetic nanoparticles, which are then delivered to the target site through an externally localized magnetic field. Therefore, the use of iron oxide magnetic nanoparticles in cancer offers the possibility of avoiding nonspecific toxicities and the promotion of a more accurate targeted dose of the anticancer agent.^{25,48} The major disadvantage of chemotherapeutic drugs is their nonspecific targeting, which increases the possibility of side effects in the healthy organs. In this context, the development of drug loading magnetic nanoparticles holds great promise.

In this work, to explore this property, two separate bottles, one containing CHO cells and the other containing MCF-7 cells, were incubated with S-nitroso-MSA-Fe₃O₄ nanoparticles at the concentration of 0.1 mg/mL for 24 h. These bottles were halfway submitted to the surface of a magnet, while the other halves were free from the influence of the magnetic field (Figure 8). As S-nitroso-MSA-Fe₃O₄ nanoparticles have superparamagnetic behaviors (Figure 4), the particles can be driven to the region under the influence of an external magnetic field.

CHO cell line, often employed in toxicity studies, was used in this experiment to verify if S-nitrosated-MSA-Fe₃O₄ could also have a toxic effect on a different cell line. As expected, cell death was only observed for cells incubated with the S-nitrosated particles under the influence of the magnetic field. Figure 8 shows the optical microscopy images for CHO and MCF-7 cells incubated with S-nitroso-MSA-Fe₃O₄ (0.1 mg/mL). The results show that for the CHO cell line, the bottle's area under the influence of the external magnetic field experienced cell death: Figure 8i and the lower section of the image in Figure 8ii. In contrast, for the CHO cell line free from the influence of the external magnetic field, no cell death was observed (Figure 8iii and the upper section of Figure 8ii). Similarly, for the MCF-7 breast cancer cell line, cell death was observed only in the area under the influence of the external magnetic field (Figure 8iv), whereas no cell death were observed in the area of the bottle free from the influence of the magnet (Figure 8v).

Taken together, these results reveal that upon the incubation of cells with S-nitrosated nanoparticles, only cells under the influence of the external magnetic field were observed to die, whereas cells free from the influence of the external magnetic field did not die. This result highlights the promising biomedical applications of S-nitrosated magnetic nanoparticles to treat cancer organs and tissues with minimal side effects to decrease the toxicity toward healthy organs.

3.6. Promising Applications of S-Nitrosated Magnetic Nanoparticles in Cancer Treatment. Taken together, our results indicate that S-nitrosated Fe₃O₄ nanoparticles, which are known as spontaneous NO donors,²⁶ have great potential to fight against cancer. There are apparently conflicting findings reported in the literature regarding the roles of NO in cancer. NO may have either pro- or antitumorigenic actions, which would depend on the NO concentration and the NO flux in a particular cellular microenvironment.⁴⁰

Overall, at low concentrations, NO acts as a protumorigenic agent, whereas at high concentrations, NO is a potent antitumorigenic agent.²⁷ For instance, increased cellular proliferation in MCF-7 cancer cells was observed upon low concentrations of NO (nanomolar range).⁴⁹ In contrast, high concentrations of NO (0.5 μmol/L NO over 24 h) were found to modulate the endogenous levels of ROS and to induce apoptosis in human breast cancer cells.^{50,51} The S-nitrosated Fe₃O₄ nanoparticles synthesized in this work were reported to spontaneously release micromolar concentrations of NO in aqueous solution,²⁶ in accordance with the anticancer effects observed in this work. The great advantage of using iron oxide magnetic nanoparticles as a vehicle to deliver NO to fight against cancer is the superparamagnetic behavior of those nanoparticles.

4. CONCLUSIONS

In this work, MSA- and DMSA-coated Fe₃O₄ superparamagnetic nanoparticles were synthesized and characterized by different techniques. Thiol groups on the surface of MSA- or DMSA-coated iron oxide magnetic nanoparticles were nitrosated, leading to the formation of S-nitroso-MSA or S-nitroso-DMSA nanoparticles. Importantly, the combination of magnetic nanoparticles with NO donor groups, such as S-nitrosated MSA or DMSA, offers new perspectives for site-specific cancer treatment.⁵²

The cytotoxicity and genotoxicity of thiolated and S-nitrosated superparamagnetic Fe₃O₄ nanoparticles were evaluated for different cell lines, including MCF-7 breast cancer cells. The results revealed that thiolated nanoparticles have low toxicity, whereas S-nitroso nanoparticles were observed to cause cytotoxic and genotoxic effects in different cell lines. Furthermore, the magnetic property of the S-nitrosated nanoparticles was used as a tool to generate a local cytotoxic effect directly at the target site of application. S-Nitrosated nanoparticles appear to constitute a potentially promising agent for the treatment of cancer and prevention of the metastatic cascade; therefore, further studies are required to clearly understand the complex and wide-ranging roles of NO to facilitate its therapeutic usage.

■ AUTHOR INFORMATION

Corresponding Author

*Exact and Earth Science Department, Universidade Federal de São Paulo, Rua São Nicolau, 210, Centro, Diadema, SP, CEP 09913030, Brazil. Phone: + 55-11-3319-3550. Fax: + 55-11-3319-3400. E-mail: amedea.seabra@unifesp.com.br.

Funding

Financial support was from FAPESP (Proc. 2012/17053-7 and 2011/10125-0), the Brazilian Network on Nanotoxicology (MCTI/CNPq).

Notes

The authors declare no competing financial interest.

■ ACKNOWLEDGMENTS

Thanks are also due to Dr. Nelson Durán (Universidade Estadual de Campinas, UNICAMP) for the use of laboratory facilities.

■ ABBREVIATIONS

DMSA, *meso*-2,3-dimercaptosuccinic acid; MSA, mercaptosuccinic acid; NO, nitric oxide; DMSO, dimethylsulfoxide; DTNB, 5',5-dithiobi(2-nitrobenzoic acid); PBS, phosphate buffered saline; XRD, X-ray diffraction; SEM, scanning electron microscopy; EDS, energy dispersive X-ray fluorescence spectrometry; VSM, vibrating sample magnetometry; PDI, polydispersity index; PCS, photon correlation spectroscopy; RPMI, Roswell Park Memorial Institute; CHO, Chinese hamster ovary; EDTA, ethylenediaminetetraacetic acid; HAECS, human aortic endothelial cells; O₂^{•-}, superoxide; ONOO⁻, peroxynitrite; NOS, nitric oxide synthase; nNOS, neuronal nitric oxide synthase; iNOS, inducible nitric oxide synthase; eNOS, endothelial nitric oxide synthase; RSNOs, S-nitrosothiols

■ REFERENCES

- (1) Seabra, A. B., and Durán, N. (2010) Nitric oxide-releasing vehicles for biomedical applications. *J. Mater. Chem.* 20, 1664–1637.
- (2) Seabra, A. B., Marcato, P. D., de Paula, L. B., and Duran, N. (2012) New strategy for controlled release of nitric oxide. *J. Nano Res.* 20, 61–67.
- (3) Seabra, A. B., and Duran, N. (2012) Nanotechnology allied to nitric oxide release materials for dermatological applications. *Curr. Nanosci.* 8, 520–525.
- (4) Seabra, A. B., and Duran, N. (2013) Biological applications of peptides nanotubes: An overview. *Peptides* 39, 47–54.
- (5) Nazir, S., Hussain, T., Ayub, A., Rashid, U., and MacRobert, A. J. (2014) Nanomaterials in combating cancer: Therapeutic applications and developments. *Nanomed. Nanotechnol.* 10, 19–34.
- (6) Haddad, P. S., and Seabra, A. B. (2012) Biomedical Applications of Magnetic Nanoparticles, in *Iron Oxides: Structure, Properties and Applications* (Martinez, A. I., Ed.) 1st ed., Vol. 1, pp 165–188, Nova Science Publishers, Inc., New York.
- (7) Chen, W., Cao, Y., Liu, M., Zhao, Q., Huang, J., Zhang, H., Deng, Z., Dai, J., Williams, D. F., and Zhang, Z. (2012) Rotavirus capsid surface protein VP4-coated Fe₃O₄ nanoparticles as a theranostic platform for cellular imaging and drug delivery. *Biomaterials* 33, 7895–7902.
- (8) Ferro-Flores, G., Ocampo-Garcia, B. E., Santos-Cuevas, C. L., Morales-Avila, E., and Azorin-Veja, E. (2014) Multifunctional radiolabeled nanoparticles for targeted therapy. *Curr. Med. Chem.* 21, 124–138.
- (9) Gajalakshmi, P., Priya, M. K., Pradeep, T., Behera, J., Kandasamy, M., Madhuwanti, S., Saran, U., and Chatterjee, S. (2013) Breast cancer drugs dampen vascular functions by interfering with nitric oxide signaling in endothelium. *Toxicol. Appl. Pharmacol.* 269, 121–131.
- (10) Cai, X. H., Wang, C. L., Chen, B. A., Hua, W. J., Shen, F., Yu, L., He, Z. M., Shi, Y. Y., Chen, Y., Xia, G. H., Cheng, J., Bao, W., Zhang, Y., and Wang, X. M. (2014) Antitumor efficacy of DMSA modified Fe₃O₄ magnetic nanoparticles combined with arsenic trioxide and adriamycin in raji cells. *J. Biomed. Nanotechnol.* 10, 251–261.
- (11) Patil, R. M., Sheta, P. B., Thorat, N. D., Otari, S. V., Barick, K. C., Prasad, A., Ningthoujam, R. S., Tiwale, B. M., and Pawar, S. H. (2014) Non-aqueous to aqueous phase transfer of oleic acid coated iron oxide nanoparticles for hyperthermia application. *RSC Adv.* 4, 4514–4522.
- (12) Lu, A. N., Salabas, E. L., and Schut, F. (2007) Magnetic nanoparticles: synthesis, protection, functionalization, and application. *Angew. Chem., Int. Ed.* 46, 1222–1244.
- (13) Auffan, M., Decome, L., Rose, J., Orsiere, T., de Meo, M., Briois, V., Chaneac, C., Olivi, L., Berge-Lefranc, J. L., Botta, A., Wiesner, M. R., and Bottero, J. W. (2006) In Vitro interactions between DMSA-coated maghemite nanoparticles and human fibroblasts: a physico-chemical and cyto-genotoxic study. *Environ. Sci. Technol.* 40, 4367–4373.
- (14) Gupta, A. K., and Gupta, M. (2005) Cytotoxicity suppression and cellular uptake enhancement of surface modified magnetic nanoparticles. *Biomaterials* 26, 1565–1573.
- (15) Brunner, T. J., Wick, P., Manser, P., Spohn, P., Grass, R. N., Limbach, L. K., Bruinink, A., and Stark, W. J. (2006) In Vitro Cytotoxicity of oxide nanoparticles: comparison to asbestos, silica, and the effect of particle solubility. *Environ. Sci. Technol.* 40, 4374–4381.
- (16) Wilhelm, C., Billotey, C., Roger, J., Pons, J. N., Bacri, J. C., and Gazeau, F. (2003) Intracellular uptake of anionic superparamagnetic nanoparticles as a function of their surface coating. *Biomaterials* 24, 1001–1011.
- (17) Jian, W., Lai, K. L., Wu, Y., and Gu, Z. W. (2014) Protein corona on magnetite nanoparticles and internalization of nanoparticle-protein complexes into healthy and cancer cells. *Arch. Pharm. Res.* 37, 129–141.
- (18) Seabra, A. B., and Haddad, P. S. (2014) Cytotoxicity and Genotoxicity of Iron Oxides Nanoparticles, in *Nanotoxicology* (Duran, N., Guterres, S., and Alves, O. L., Eds.) 1st ed., Vol. 1, pp 265–280, Springer, New York.
- (19) Liu, Y. X., and Wang, J. K. (2011) Comparative and quantitative investigation of cell labeling of a 12-nm DMSA-coated Fe₃O₄ magnetic nanoparticle with multiple mammalian cell lines. *J. Mater. Res.* 26, 822–831.
- (20) Mejias, R., Gutierrez, L., Salas, G., Perez-Yague, S., Zotes, T. M., Lazaro, F. J., Morales, M. P., and Barber, D. F. (2013) Long term biotransformation and toxicity of dimercaptosuccinic acid-coated magnetic nanoparticles support their use in biomedical applications. *J. Controlled Release* 171, 225–233.
- (21) Ge, G., Wu, H., Xiong, F., Zhang, Y., Guo, Z., Bian, Z., Xu, J., Gu, C., Gu, N., Chen, X., and Yang, D. (2013) The cytotoxicity evaluation of magnetic iron oxide nanoparticles on human aortic endothelial cells. *Nanoscale Res. Lett.* 8, 215.
- (22) Liu, Y., Chen, Z., Gu, N., and Wang, J. (2011) Effects of DMSA-coated Fe₃O₄ magnetic nanoparticles on global gene expression of mouse macrophage RAW264.7 cells. *Toxicol. Lett.* 205, 130–139.
- (23) de Lima, R., Oliveira, J. L., Ludescher, A., Molina, M. M., Itri, R., Seabra, A. B., and Haddad, P. S. (2013) Nitric oxide releasing iron oxide magnetic nanoparticles for biomedical applications: cell viability, apoptosis and cell death evaluations. *J. Phys. Conf. Ser.* 429, 012034.
- (24) de Lima, R., Oliveira, J. L., Murakami, P. S. K., Molina, M. M., Itri, R., Haddad, P. S., and Seabra, A. B. (2013) Iron oxide nanoparticles show no toxicity in the comet assay in lymphocytes: A promising vehicle as a nitric oxide releasing nanocarrier in biomedical applications. *J. Phys. Conf. Ser.* 429, 012021.
- (25) Dilnawaz, F., Singh, A., Mohanty, C., and Sahoo, S. (2010) Dual drug loaded superparamagnetic iron oxide nanoparticles for targeted cancer therapy. *Biomaterials* 31, 3694–3706.
- (26) Molina, M. M., Seabra, A. B., de Oliveira, M. G., Itri, R., and Haddad, P. S. (2013) Nitric oxide donor superparamagnetic iron oxide nanoparticles. *Mater. Sci. Eng. C* 33, 746–751.
- (27) Ignarro, L. J. (2000) *Nitric Oxide: Biology and Pathobiology*, Academic Press, Waltham, MA.
- (28) Lei, J., Vodovotz, Y., Tzeng, E., and Billiar, T. R. (2013) Nitric oxide, a protective molecule in the cardiovascular system. *Nitric Oxide* 35, 175–185.
- (29) Georgii, J. L., Amadeu, T. P., Seabra, A. B., de Oliveira, M. G., and Costa, A. M. A. (2011) Topical S-nitrosoglutathione-releasing hydrogel improves healing of rat ischaemic wounds. *J. Tissue Eng. Regener. Med.* 5, 612–619.
- (30) Seabra, A. B., Pankotai, E., Fehér, M., Somlai, A., Kiss, L., Bíró, L., Szabó, C., Kollai, M., de Oliveira, M. G., and Lacza, Z. (2007) S-nitrosoglutathione-containing hydrogel increases dermal blood flow in streptozotocin-induced diabetic rats. *Br. J. Dermatol.* 156, 814–818.

- (31) Seabra, A. B., da Silva, R., de Souza, G. F. P., and de Oliveira, M. G. (2008) Antithrombogenic polynitrosated polyester/poly(methyl methacrylate) blend for the coating of blood-contacting surfaces. *Artif. Organs* 32, 262–267.
- (32) Seabra, A. B., Martins, D., Simões, M. M. S. G., da Silva, R., Brocchi, M., and de Oliveira, M. G. (2010) Antibacterial nitric oxide-releasing polyester for the coating of blood-contacting artificial materials. *Artif. Organs* 34, E204–E214.
- (33) Choudhari, S. K., Chaudhary, M., Bagde, S., Gadbail, A. R., and Josh, V. (2013) Nitric oxide and cancer: a review. *World J. Surg. Oncol.* 11, 118.
- (34) Carpenter, A. W., and Schoenfisch, M. H. (2012) Nitric oxide release: Part II. Therapeutic applications. *Chem. Soc. Rev.* 41, 3742–3752.
- (35) Chandra, S., Nigam, S., and Bahadur, D. (2014) Combining unique properties of dendrimers and magnetic nanoparticles towards cancer theranostics. *J. Biomed. Nanotechnol.* 10, 32–49.
- (36) de Lima, R., Feitosa, L. O., Maruyama, C. R., Barga, M. A., Yamawaki, P. C., Vieira, I. J., Teixeira, E. M., Corrêa, A. C., Mattoso, L. H. C., and Fraceto, L. F. (2012) Evaluation of the genotoxicity of cellulose nanofibers. *Int. J. Nanomed.* 7, 3555–3565.
- (37) de Oliveira, M. G., Shishido, S. M., Seabra, A. B., and Morgan, N. H. (2002) Thermal stability of primary S-nitrosothiols: Roles of autocatalysis and structural effects on the rate of nitric oxide release. *J. Phys. Chem. A* 106, 8963–8970.
- (38) Shishido, S. M., Seabra, A. B., Loh, W., and de Oliveira, M. G. (2003) Thermal and photochemical nitric oxide release from S-nitrosothiols incorporated in pluronic F127 gel: potential uses for local and controlled nitric oxide release. *Biomaterials* 24, 3543–3553.
- (39) Huerta, S., Chilka, S., and Bonavida, B. (2008) Nitric oxide donors: Novel cancer therapeutics (Review). *Int. J. Oncol.* 33, 909–927.
- (40) Burke, A. J., Sullivan, F. J., Giles, F. J., and Glynn, S. A. (2013) The yin and yan of nitric oxide in cancer progression. *Carcinogenesis* 34, 503–512.
- (41) Leon, L., Jeannin, J. F., and Bettaieb, A. (2008) Post-translational modifications induced by nitric oxide (NO): Implication in cancer cells apoptosis. *Nitric Oxide* 19, 77–83.
- (42) Xie, K., and Huang, S. (2003) Contribution of nitric oxide-mediated apoptosis to cancer metastasis inefficiency. *Free Radical Biol. Med.* 34, 969–986.
- (43) Li, C. Q., and Wogan, G. N. (2005) Nitric oxide as a modulator of apoptosis. *Cancer Lett.* 226, 1–15.
- (44) Melino, G., Catani, M. V., Corazzari, P., and Bernassola, F. (2000) Nitric oxide can inhibit apoptosis or switch it into necrosis. *Cell. Mol. Life Sci.* 57, 612–622.
- (45) Muntané, J., de la Rosa, A. J., Marín, L. M., and Padillo, F. J. (2013) Nitric oxide and cell death in liver cancer cells. *Mitochondrion* 13, 257–262.
- (46) Collins, A. R., Oscoz, A. A., Brunborg, G., Gaivao, I., Giovannelli, L., Kruszewski, M., Smith, C. C., and Stetina, R. (2008) The comet assay: topical issues. *Mutagenesis* 23, 143–151.
- (47) Li, J., and Billiar, T. R. (2000) The role of nitric oxide in apoptosis. *Semin. Perinatol.* 24, 46–50.
- (48) Jain, T. K., Morales, M. A., Sahoo, S. K., Leslie-Pelecky, D. L., and Labhsetwar, V. (2005) Iron oxide nanoparticles for sustained delivery of anticancer agents. *Mol. Pharmaceutics* 2, 194–205.
- (49) Pervin, S., Singh, R., Hernadez, E., Wu, G. Y., and Chaudhuri, G. (2007) Nitric oxide in physiologic concentrations targets the translational machinery to increase the proliferation of human breast cancer cells: involvement of mammalian target of rapamycin/eIF4E pathway. *Cancer Res.* 67, 289–299.
- (50) Sen, S., Kawahara, B., Fukuto, J., and Chaudhuri, G. (2013) Induction of a feed forward pro-apoptotic mechanistic loop by nitric oxide in a human breast cancer model. *PLoS One* 8, e70693.
- (51) Sen, S., Kawahara, B., and Chaudhuri, G. (2013) Mitochondrial-associated nitric oxide synthase activity inhibits cytochrome c oxidase: Implications for breast cancer. *Free Radical Biol. Med.* 57, 210–220.
- (52) Seabra, A. B., Haddad, P. S., and Duran, N. (2013) Biogenic synthesis of nanostructured iron compounds: applications and perspectives. *IET Nanobiotechnol.* 7, 90–99.